Power Electronic Systems
Laboratory

© 2022 IEEE

Proceedings of the IEEE International Ultrasonic Symposium (IUS 2022), Venice, Italy, October 11-13, 2022

Contactless Positioning of Objects on Acoustically Reflective Surfaces by Means of Ultrasonic Forces

M. Röthlisberger,
T. Wilhelm,
M. Schuck,
J. W. Kolar

Personal use of this material is permitted. Permission from IEEE must be obtained for all other uses, in any current or future media, including reprinting/republishing this material for advertising or promotional purposes, creating new collective works, for resale or redistribution to servers or lists, or reuse of any copyrighted component of this work in other works

Eidgenössische Technische Hochschule Zürich
Swiss Federal Institute of Technology Zurich

Contactless Positioning of Objects on Acoustically Reflective Surfaces by Means of Ultrasonic Forces

Marc Röthlisberger
Power Electronic Systems Laboratory
ETH Zurich
Zurich, Switzerland
roethlisberger@lem.ee.ethz.ch

Timo Wilhelm
Power Electronic Systems Laboratory
ETH Zurich
Zurich, Switzerland
twilhelm@student.ethz.ch

Marcel Schuck
Power Electronic Systems Laboratory
ETH Zurich
Zurich, Switzerland
schuck@lem.ee.ethz.ch

Johann W. Kolar
Power Electronic Systems Laboratory
ETH Zurich
Zurich, Switzerland
kolar@lem.ee.ethz.ch

***Abstract*—Ultrasonic forces have been used to keep small objects in a suspended state for a long time. In recent years, methods have been developed to manipulate the levitating objects and to lift objects located on acoustically transparent or reflective surfaces. This work demonstrates an ultrasonic levitation system, which is capable of transporting objects from and to acoustically reflective surfaces, while controlling the orientation of the levitating object. This requires two different types of piezoelectric transducers operating at two distinct frequencies (25 kHz and 40 kHz), a moveable reflector plate and a novel control method. With these properties, the levitation system presented in this work can be used as a precise contact-less robotic gripper for micro-manufacturing processes of small and fragile objects.**

***Index Terms*—Acoustic Levitation, Ultrasonic Grippers, Robotics**

I. Introduction

Ultrasonic forces are used to trap small objects or liquids in chemistry [1], control of nano material self-assembly [2], containerless processing [3]–[6], and to study droplet dynamics [7], [8].

A single transducer and a reflector are sufficient to create a standing wave that can levitate an object [9]. In recent years, arrays of ultrasonic transducers have been used not only to levitate but also to manipulate small objects and liquids [10]–[12].

To use this technology for robotic grippers, it has to be possible to pick up objects located in different environments, transport them reliably and position the objects on a target. A method for the transport from and to acoustically reflective surfaces has previously been developed [3]. Due to the symmetry of the pressure field resulting from this method, the object levitating in the gripper had the tendency to spin around the symmetry axis of the gripper and was therefore not in a controlled state.

It has been shown, that the superposition of pressure fields and force potentials generated by transducers operating at different frequencies can be calculated separately and added up to get the total pressure field and force potential [13], [14]. This method was used for the gripper developed in this work in order to generate a stabilizing torque which stops the spin of levitating asymmetric objects. The torque can be adjusted such that the orientation of the levitating object can not only be stabilized but also controlled. Therefore, it is possible to position the object on a target surface in a precise manner, which is required for any micro manufacturing process using ultrasonic grippers.

II. Methods

The acoustic pressure generated by the j^{th} transducer of an acoustic array at a given point in space is calculated as

$$p_j = e^{i\phi} P_0 J_0(kr \sin\theta) \frac{1}{d} e^{ikd}, \tag{1}$$

where ϕ, P_0, J_0, d, θ, r and $k = \omega/c_0$ denote the phase of the transducer excitation signal, a factor depending on the electrical power ($P_0 = 0.13\,V_{\text{ex}}$ [15]), the Bessel function of order zero, the distance of the considered point to the transducer, the beam angle, the radius of the transducer, and the wave number, respectively [10].

An approximation for the force potential valid for objects smaller than the acoustic wavelength ($\lambda \approx 8.65\,\text{mm}$) is the Gor'kov potential U. It is calculated as

$$U = V_{\text{p}} \left(K_1 \langle P^2 \rangle - K_2 \langle V^2 \rangle \right), \tag{2}$$

with $\langle\rangle$, V_{p}, P, and V denoting time-averaged terms, the particle volume, the pressure, and the particle velocity, respectively. K_1 and K_2 denote factors that depend on the density of the levitating object and the medium as well as the speed of sound in the levitating object and the medium (air) [10].

The ultrasonic gripper presented in this work uses piezoelectric transducers operating at $40\,\text{kHz}$ and $25\,\text{kHz}$. The $40\,\text{kHz}$ transducers are used to counteract the gravitational force. This is achieved by arranging them on a spherical cap with a radius of $r = 42\,\text{mm}$ and operating all transducers at the same phase. If an acoustically reflective surface is placed near the

focus point of the arrangement, a standing wave between the gripper and the reflective surface is formed, as shown in Fig. 1b. Objects located on the reflective surface can be picked up using this method, since they are pushed towards the first pressure minimum, which is about a quarter of a wavelength ($\frac{\lambda}{4} \approx 2.15\,\mathrm{mm}$) above the surface.

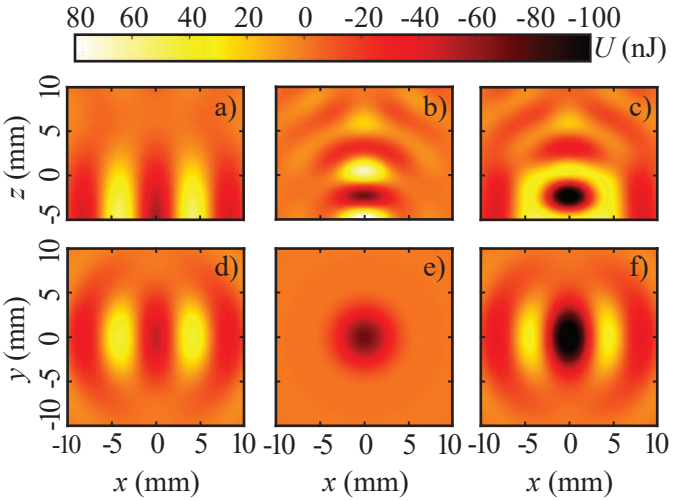

Fig. 1. Side and top view of the Gor'kov potential resulting from the transducers operating at (a), (d) 25 kHz, (b), (e) 40 kHz and (c), (f) the combination of both. The focus point of the gripper is at $x, y, z = 0\,\mathrm{mm}$ and the a reflective surface is located at $z = -5\,\mathrm{mm}$. The asymmetry of the pressure field shown in (f) is required for stabilizing the orientation of the levitating object. The potentials in (a), (b), and (c) are shown for $y = 0\,\mathrm{mm}$ and the potentials in (d), (e), and (f) are shown for $z = 2.15\,\mathrm{mm}$.

When the object is levitating in this pressure minimum, a thin reflector plate can be moved under the levitating object, resulting in a standing wave between the transducers and the reflector plate. The 3d printed reflector plate with a thickness of $t = 0.8\,\mathrm{mm}$ is placed $5\,\mathrm{mm}$ below the focus point of the gripper in order to have enough space for the 25 kHz transducers. A slope was added to the edges of the plate to reduce disturbances of the pressure field during the movement of the reflector plate. The gripper (including the reflector plate) can then be moved away from the reflective surface while maintaining stable levitation [3].

Objects levitating in this gripper tend to spin around the symmetry axis, due to the symmetrical pressure field [3], [16]–[18]. A ring shaped arrangement ($r = 53\,\mathrm{mm}$) of transducers operating at 25 kHz is used to superimpose an asymmetric pressure field, that provides a stabilizing torque. As shown in [13], the superimposed pressure and force potential field can be calculated as the sum of the 40 kHz and the 25 kHz pressure and force potential fields. Due to the lack of space, the transducers were only arranged on two sides of the gripper and not in a full circle. The gripper including the reflector plate is shown in Fig. 2. The resulting asymmetric Gor'kov potential, the 40 kHz Gor'kov potential and the 25 kHz Gor'kov potential are shown in Fig. 1.

This system is not only capable of transporting asymmetric

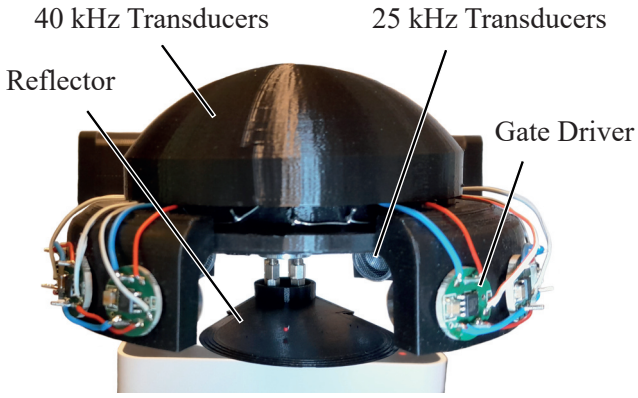

Fig. 2. The gripper used to verify the presented methods.

objects in a fixed position but it is also possible to control the orientation of the levitating object. By controlling the phase shifts of the 25 kHz transducers individually, it is possible to rotate the 25 kHz pressure field and therefore the object around the z-axis. For the initial position, a phase shift of 180 ° between the two halves of the 25 kHz arrangement is applied. By adjusting which transducers are operating at 0 ° and 180 ° phase, the pressure field can be rotated as illustrated in Fig. 5. For smoother rotation, the phase shift of the transducers can be increased gradually from 0 ° to 180 ° and vice versa.

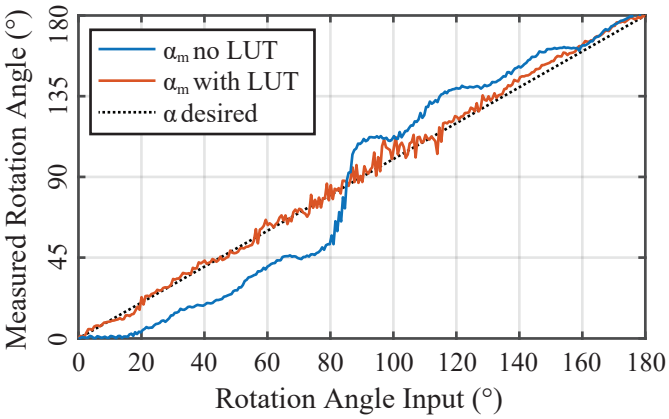

Fig. 3. Measured rotation angle α_m for 10 V and 8 V excitation voltage amplitudes for the transducers operating at 40 kHz and 25 kHz, respectively. The blue line shows the trajectory using the simple phase calculating method and the red line uses a look up table measured for this combination of excitation voltages.

For placing the object on a target on a reflective surface, the same method as for the picking process can be used. The gripper can be moved to the target surface, such that the reflector is very close to the surface. By removing the reflector and reducing the acoustic power afterwards, the object can be placed on the target in a controlled manner.

The gripper is mounted on a robotic arm to allow long distance movement of the objects. The arm and the stepper motor, which is used to move the reflector plate, are controlled

by a Raspberry Pi, which also calculates the required phase shifts and duty cycles for the transducers and forwards them to a Cyclone IV FPGA board. The FPGA generates one signal for each transducer operating at 25 kHz, which is inverted and amplified by one gate driver IC per transducer (IX4428). This is required for individually controlling the phase shifts of the transducers and allow the rotation of the levitating object. Additionally, two signals for the transducers operating at 40 kHz are generated on the FPGA and are amplified by an L298N dual H-bridge board. An overview of the system is shown in Fig. 4.

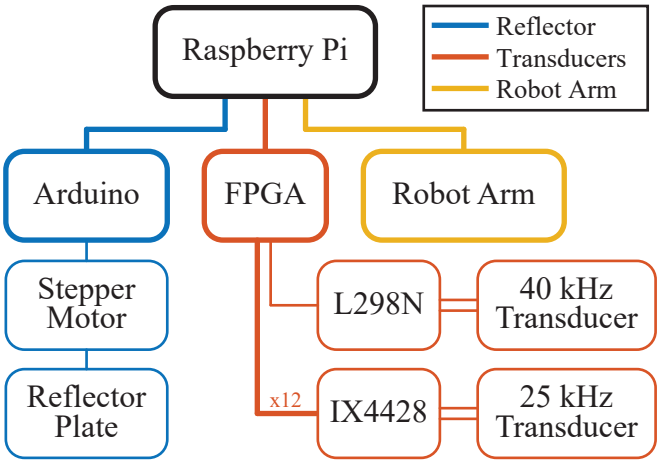

Fig. 4. Overview of the components used to control the gripper. The robot arm and the stepper motor, which is used to move the reflector plate, are controlled by a Raspberry Pi, which also calculates the required phase shifts and duty cycles for the transducers and forwards them to a Cyclone IV FPGA board. The FPGA generates one signal for each transducer operating at 25 kHz, which is inverted and amplified by one gate driver IC per transducer (IX4428). Additionally, two signals for the transducers operating at 40 kHz are generated on the FPGA and are amplified by an L298N dual H-bridge board.

III. Results

The methods presented in this work facilitate the reliable transport of small and fragile objects located on acoustically reflective surfaces, if the gripper is positioned precisely above the object. For objects with high density ($\rho \geq 1\,\mathrm{g/cm^3}$), some oscillations occur during the picking process. The added slope to the edge of the reflector plate reduces the disturbances of the pressure field during the movement of the reflector plate significantly and improve the stability during the picking process.

The stabilization of asymmetric objects with piezoelectric transducers operating at 25 kHz requires a suitable choice of operating voltages. If the operating voltage is chosen too low, the stabilizing torque is too weak in order to stop the rotation of the particle. However, for very high operating voltage, the particle tilts around the horizontal axis with the lowest stiffness or even starts to wobble around this axis, when the horizontal and vertical forces are of similar strength. The operating voltages, which yielded the best stability during our experiments are shown in table I. With suitable operating voltages, the object can be kept in a stable position even during the movement of the robotic arm, which causes vibrations of the gripper.

TABLE I
Best suited operating voltages (RMS) for the transducers operating at 25 kHz and 40 kHz and different materials.

Material	40 kHz Voltage	25 kHz Voltage
Styrofoam	10 V	8 V
PLA	19 V	16.5 V
Tin	25 V	20 V

The orientation angle α of the object should not be changed before arriving at the target location since the initial orientation ($\alpha = 0°$) is the most stable as shown in Fig. 5. The simplest approach for calculating the phase shifts for the transducers operating at 25 kHz is

$$\varphi_j = \begin{cases} 180° & \alpha_j > 210° \\ 6(\alpha_j - 180°) & 180° < \alpha_j \leq 210° \\ 0° & 30° < \alpha_j \leq 180° \\ 6\alpha_j + 180° & \text{otherwise} \end{cases} \quad (3)$$

where $\alpha_j = \alpha + j \cdot 30°$ is the rotation angle relative to the j-th transducer and assuming uniformly distributed transducers. This approach results in smooth phase shift changes for each transducer. As shown in Fig. 3, there is a deviation between the measured orientation angle α_m and the input angle α. Two kinds of deviations occur during a revolution. First, the non uniform distribution of the transducers causes a slower rotation for the largest part of the revolution and a faster rotation for rotation angles around 90°. Furthermore, the linear phase shift change of each transducer from 0° to 180° results in a non linear orientation angle change during each 30° rotation interval. Both kinds of deviation can be compensated for by a lookup table for fixed operating voltages as shown in Fig. 3. The lookup table was generated using video footage and openCV image processing algorithms for the rotation angle detection. For slight deviations of operating voltages, which are often required for objects of different shape, the lookup table can still be used with small orientation inaccuracy. For objects of different materials, the operating voltages differ too much from the ones used for the lookup table and relatively large inaccuracies can occur. Therefore, we recommend to use an individual lookup table for each material.

IV. Discussion

This work presents the first ultrasonic robotic gripper, which allows the contactless transport of small and fragile objects in a controlled manner. Its capability of controlling the orientation of levitating objects is required for applications in micro-manufacturing processes. With the presented methods, high positioning and orientation accuracy can be achieved. Oscillations during the picking process and the movement of the robotic arm limit the stability and reliability of the transport and should therefore be further reduced in future research.

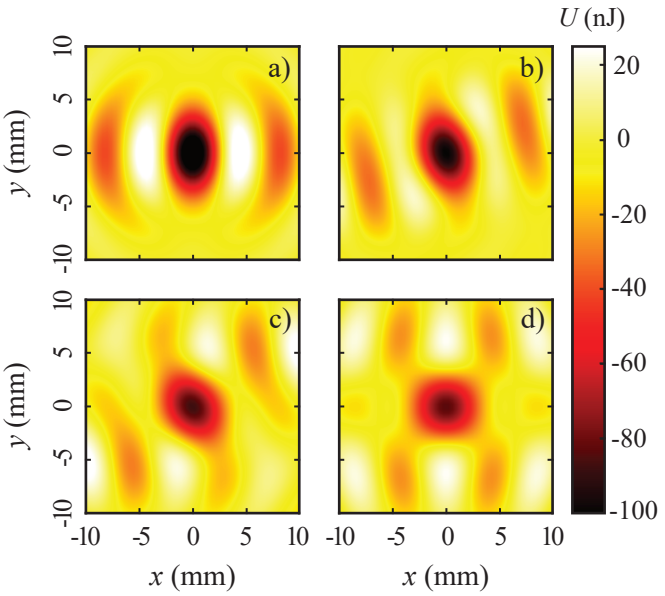

Fig. 5. Top view of the Gor'kov potential for rotation angles of (a) 0°, (b) 30°, (c) 45° and (d) 90°.

There is still potential for improvement in gripper design, since this work has focused on methods rather than gripper optimization. If very high positioning accuracy is required, the system can be extended with a closed-loop control system using the image processing algorithms used for the lookup table generation.

ACKNOWLEDGMENTS

This research was supported by Arbeitsgemeinschaft Prof. Hugel and the ETH Zurich Foundation.

REFERENCES

[1] S. Santesson and S. Nilsson, "Airborne chemistry: Acoustic levitation in chemical analysis," *Analytical and bioanalytical chemistry*, vol. 378, pp. 1704–1709, may 2004.

[2] A. M. Seddon, S. J. Richardson, K. Rastogi, T. S. Plivelic, A. M. Squires, and C. Pfrang, "Control of Nanomaterial Self-Assembly in Ultrasonically Levitated Droplets," *The Journal of Physical Chemistry Letters*, vol. 7, no. 7, pp. 1341–1345, apr 2016. [Online]. Available: https://doi.org/10.1021/acs.jpclett.6b00449

[3] M. Röthlisberger, M. Schuck, L. Kulmer, and J. Kolar, "Contactless picking of objects using an acoustic gripper," *Actuators*, vol. 10, p. 70, 03 2021.

[4] D. Foresti, G. Sambatakakis, S. Bottan, and D. Poulikakos, "Morphing Surfaces Enable Acoustophoretic Contactless Transport of Ultrahigh-Density Matter in Air," *Scientific Reports*, vol. 3, no. 1, p. 3176, 2013. [Online]. Available: https://doi.org/10.1038/srep03176

[5] P. C. Nordine, D. Merkley, J. Sickel, S. Finkelman, R. Telle, A. Kaiser, and R. Prieler, "A levitation instrument for containerless study of molten materials," *Review of Scientific Instruments*, vol. 83, no. 12, p. 125107, dec 2012. [Online]. Available: https://doi.org/10.1063/1.4770125

[6] N. Yan, Z. Y. Hong, D. Geng, and B. Wei, "A comparison of acoustic levitation with microgravity processing for containerless solidification of ternary Al–Cu–Sn alloy," *Applied Physics A*, vol. 120, apr 2015.

[7] K. Ohsaka and E. Trinh, "Three-Lobed Shape Bifurcation of Rotating Liquid Drops," *Physical review letters*, vol. 84, pp. 1700–1703, mar 2000.

[8] C. Shen, W. Xie, and B. Wei, "Parametrically excited sectorial oscillation of liquid drops floating in ultrasound," *Physical review. E, Statistical, nonlinear, and soft matter physics*, vol. 81, p. 46305, apr 2010.

[9] A. Kundt, "Über eine neue Art akustischer Staubfiguren und über die Anwendung derselben zur Bestimmung der Schallgeschwindigkeit in festen Körpern und Gasen," *Annalen der Physik*, no. 203.4, p. 497–523, 1866.

[10] A. Marzo, S. A. Seah, B. W. Drinkwater, D. R. Sahoo, B. Long, and S. Subramanian, "Holographic acoustic elements for manipulation of levitated objects," *Nat. Commun.*, vol. 6, p. 8661, 2015.

[11] M. Röthlisberger, M. Schuck, and J. W. Kolar, "Kilohertz-frequency rotation of acoustically levitated particles," *IEEE Transactions on Ultrasonics, Ferroelectrics, and Frequency Control*, vol. 69, no. 4, pp. 1528–1534, 2022.

[12] A. Marzo, T. Corkett, and B. W. Drinkwater, "Ultraino: An open phased-array system for narrowband airborne ultrasound transmission," *IEEE Transactions on Ultrasonics, Ferroelectrics, and Frequency Control*, vol. 65, no. 1, pp. 102–111, 2018.

[13] M. Röthlisberger, G. Schmidli, M. Schuck, and J. W. Kolar, "Multi-frequency acoustic levitation and trapping of particles in all degrees of freedom," *IEEE Transactions on Ultrasonics, Ferroelectrics, and Frequency Control*, vol. 69, no. 4, pp. 1572–1575, 2022.

[14] T. Puranen, P. Helander, A. Meriläinen, G. Maconi, A. Penttilä, M. Gritsevich, I. Kassamakov, A. Salmi, K. Muinonen, and E. Hæggström, "Multifrequency acoustic levitation," in *2019 IEEE International Ultrasonics Symposium (IUS)*, 2019, pp. 916–919.

[15] A. Marzo, A. Barnes, and B. W. Drinkwater, "Tinylev: A multi-emitter single-axis acoustic levitator," *Review of Scientific Instruments*, vol. 88, no. 8, p. 085105, 2017. [Online]. Available: https://doi.org/10.1063/1.4989995

[16] T. Schwarz, P. Hahn, G. Petit-Pierre, and J. Dual, "Rotation of fibers and other non-spherical particles by the acoustic radiation torque," *Microfluidics and Nanofluidics*, vol. 18, no. 1, pp. 65–79, 2015. [Online]. Available: https://doi.org/10.1007/s10404-014-1408-9

[17] V. Vandaele, A. Delchambre, and P. Lambert, "Acoustic wave levitation: Handling of components," *J. Appl. Phys.*, vol. 109, p. 124901, 2011.

[18] Q. Xiu-Pei, G. De-Lu, H. Zhen-Yu, and W. Bing-Bo, "Rotation mechanism of ultrasonically levitated cylinders," *Acta Phys. Sin.*, vol. 66, p. 124301, 2017.